International Journal of Engineering Research & Technology (IJERT)
ISSN: 2278-0181
Vol. 4 Issue 08, August-2015

Mechanical Property of Parallel Polyvinyl Alcohol Nanofibers Reinforced by MWCNTs, and its Composites

Xinnan Wang, and Marshall Mcnea,
Department of Mechanical Engineering
North Dakota State University
Fargo, ND, USA 58108

***Abstract* - In this paper, electrospinning was used to create parallel polyvinyl alcohol (PVA) MWCNTs nanofibers. Epoxy composites reinforced by PVA array and PVA/MWCNTs array were fabricated, respectively. Mechanical characterization was performed. Through AFM analysis, the morphology of the PVA fiber was much smoother and more uniform than the MWCNT/PVA fiber. The elastic moduli and hardness of PVA and MWCNT/PVA fibers from Nanoindentation tests were calculated. The 15 wt% MWCNTs exhibited significant improvement in the mechanical property. Tensile testing shows that the epoxy sample reinforced with the MWCNT/PVA parallel fiber arrays had the highest tensile strength, followed by the plain epoxy control sample, and the epoxy reinforced with PVA parallel fiber array. It was postulated that the addition of the PVA fiber arrays in the epoxy matrix weakens the overall mechanical property of the composite. The elongation at break for the epoxy reinforced with the MWCNT/PVA parallel fiber arrays was decreased compared with the failure strain of the plain epoxy. It indicated that the incorporation of MWCNTs in the epoxy matrix creates composites with higher modulus and strength, especially with the array of parallel reinforcing nanofibers in the matrix.**

INTRODUCTION

Polymeric materials play an essential role in everyday life due to their wide range of properties and manufacturability. There has been intensive research focus on polymer nanocomposites to tailor their mechanical properties.[1-4] The properties of the resulting polymer composites highly depend on the properties, geometry, weight percentage, dispersion, and spatial orientation of the nano reinforcements, etc., [5, 6] among which carbon nanotube (CNT) has been an excellent one-dimensional nano reinforcement material due to its remarkable structural, chemical, electrical, and mechanical properties and performance.[5, 7-10]

Electrospinning is a versatile technique that enables mass production of long nano polymer fibers with a diameter range of 50 nm up to a few micrometers. This technique has been successfully used in drug delivery,[11] biological scaffolds in tissue engineering,[12, 13] filtering medium,[12, 14] and textile applications.[15] The principle is that a polymer solution droplet on a capillary tip is stretched with an introduction of an electric field to form a Taylor cone[16]. When the electric field is sufficiently strong, a charged jet of the polymer solution is ejected out of the cone tip. The continuous charged nanofibers can be created by the whipping elongation of the liquid polymer jet,[17] and form randomly orientated mats on a metal collector frame.[18] The jet trajectory can be controlled by an extra electric field at the collector. With the collector properly designed and configured, and addition of nanofillers in the polymer solution, patterned nanocomposites fibers mat can be synthesized. [18-26] Parallel fibers can be fabricated by two parallel plates [27] or a tower collector. [28] Both designs use grounded parallel collectors to achieve aligned fibers which related to the manufacture of the plate design used to create fibers for this set up.

As presented by Ge *et al*. the electrospinning of MWCNT has been accomplished with polyacrylonitrile as the polymer. [29] The importance of this study proves that MWCNT can be placed into polymer sample in a highly aligned method. As multi-walled carbon nanotubes (MWCNTs) are less costly to produce, our study was to use MWCNT to create composites where MWCNTs were aligned. No functionalization treatments on the MWCNTs were used. Electrospun polyvinyl alcohol (PVA) fibers were to be used to orientate the MWCNTs while providing a matrix in which they could be held in a parallel alignment. This would allow for the fibers to be placed into a mold before the epoxy would be introduced into the mold.

2. MATERIALS AND METHODS

Materials Fabrication

The purchased materials included PVA (M_w ≈60 kDa, 98% hydrolyzed) from Sigma-Aldrich, as received MWCNTs (outer diameter: > 50 nm, length: 10-20 μm) with purity of >95% from Cheap Tubes Inc., and long cure epoxy with associated hardener from Leco Co. as composite matrix. Deionized water (18 MΩ·cm at 22°C) was produced from a Millipore Purification System (EMD Millipore).

Parallel nanofibers was produced by the home-made electrospinner, schematically illustrated in Fig. 1. The setup consisted of a syringe with a metallic needle (Analytical West, Inc.), a syringe pump (Legato 100, KD Scientific, not drawn), a Gamma high-voltage DC power supply, and a grounded U-shape aluminum plate collector. The collector was machined with five pairs of rectangular teeth having an opening gap of 5 cm insulating gap, each tooth was 1 cm

wide and the gap between the neighboring teeth was 1.5 cm. The collector was put 12 cm under the needle tip. The main control parameters for electrospinning included viscosity of the solution, the syringe pumping rate, and voltage. The viscosity was altered by using different concentrations of PVA in the water solution so that uniform structured fibers was finally fabricated. In a typical experiment, 15 wt.% PVA aqueous solution was prepared, the pumping rate was 3 μL/min, and the applied voltage was10 kV. To dissolve PVA and retain the water percentage in a media jar, the jar was tightly capped and immersed in a beaker of water, and magnetically stirred on a heating stage. A ceramic spacer was put between the media jar and the beaker to avoid excessive heat to PVA on the bottom of the jar. The solution was stirred until complete PVA dissolution.[30-32] The heating temperature was then gradually reduced from 95 °C to 85 °C and kept for one hour; meanwhile the solution was continuously stirred for two hours at a lower speed to prevent PVA from clumping and introducing air bubbles into the solution. The same procedure was applied to the MWCNT/PVA solution, except that 1 wt.% MWCNTs were added in the PVA solution and ultra sonicated for 45 min. Parallel fibers were electrospun and collected across the teeth gaps in a humidity-controlled plastic chamber.

For fabrication of epoxy composites reinforced by parallel PVA and MWCNT/PVA fibers, respectively, a dog-bone shaped sample mold with epoxy matrix (epoxy to hardener volume ratio was 3:1) was put under the collector and aligned with the teeth gap direction. A thick layer of fiber arrays were embedded in the epoxy. Figure 2 shows the dimensions of a dog-bone shaped sample. Three types of specimens were fabricated for mechanical property comparison: plain epoxy as the control sample, parallel PVA fiber reinforced epoxy composite, and epoxy with parallel MWCNT/PVA fibers reinforcements.

TESTING METHODS

To investigate the topography, geometry and parallelizability of the PVA and MWCNT/PVA fibers, an atomic force microscope (AFM, Dimension 3100, Bruker Co.) was used to image the electrospun fibers that were collected on a glass slide.

Prior to the mechanical property comparison of the composite samples, the elastic moduli of the PVA and MWCNT/PVA fibers were studied by nanoindentation using a Hysitron TI 950 TriboIndenter. Due to the weak adhesion between the fiber and the glass slide, electro-beam-induced deposition (EBID)[33] technique was applied to fix the fibers on the substrate at 1 μm intervals to prevent the fiber from sliding during indentation.

The indentation load and displacement of the Berkovich indenter tip was recorded during indentation with a force resolution of less than 1 nN and displacement resolution of 0.02 nm. The 50 nm-radius indenter tip imaged a fiber, pinpointed the top surface of the fiber, and then make indentations *in situ*. Based on the Oliver-Pharr method,[34] the unloading stiffness was first obtained from the slope of the initial portion of the unloading curve. Based on Sneddon's method,[35] the relation between contact stiffness S, contact area A, and reduced elastic modulus E_r is:

$$S = 2\beta\sqrt{\frac{A}{\pi}}E_r \quad (1)$$

where β is a geometry factor depending on the indenter tip shape (β = 1.034 for a Berkovich indenter).[34] The reduced elastic modulus is the effective modulus combining the moduli of the indenter tip and the specimen according to

$$\frac{1}{E_r} = \frac{1-\nu_f^2}{E_f} + \frac{1-\nu_i^2}{E_i} \quad (2)$$

where E and ν represent the elastic modulus and Poisson's ratio, respectively. The subscripts i and f denote the indenter and fiber, respectively. For the diamond tip, E_i = 1140 GPa, ν_i = 0.07.[34] ν_f=0.45 was used for both PVA and MWCNT/PVA fibers.

From the load-displacement curve, the contact depth h_c was obtained by

$$h_c = h_{max} - \epsilon\frac{F_{max}}{S} \quad (3)$$

where ϵ is another indenter tip geometry factor (ϵ = 0.75 for a Berkovich indenter), h_{max} and F_{max} are the maximum displacement and indentation force, respectively.

From the load *v.s.* displacement curve, nanoindentation hardness can be obtained as

$$H = \frac{F_{max}}{A} \quad (4)$$

where F_{max} is the peak load, A is the projected contact area. Ten indentation tests were performed for each MWCNT/PVA fiber and PVA fiber.

Uniaxial tensile tests were conducted on each composite sample with an in-house designed micro tensile tester. The tester has the displacement resolution of 33.2 nm, and the travel range is up to 57 mm. The strain rate was set at 0.001 s^{-1}. All specimens were strained to failure. The loading force *v.s.* sample elongation were recorded for subsequent mechanical property analyses. Ten specimens were tested for each sample.

RESULTS AND DISCUSSION

Both pure PVA and MWCNT/PVA nanofibers were successfully fabricated by electrospinning. Figure 3 shows an AFM height image of an array of electrospun fibers on a glass substrate after 2 seconds of electrospinning. It suggests the collector design enables a high degree of fiber parallelism. The charges on the fibers, when approaching the vicinity of the electrodes after being ejected, induce opposite charges from the electrode surface, which increase the attraction force between the fibers and the electrodes as the separation becomes smaller. As a result, the fibers are led to uniaxial alignment across the teeth gaps.[36, 37]

AFM was used to observe the morphology of the nanofibers. The tapping mode height images of the two representative fibers in Fig. 4a&b show that the PVA fiber has a much smoother morphology and a more uniform diameter than that of the MWCNT/PVA fiber. No individual MWCNTs were found on the fiber surface, indicating the MWCNTs were well embedded within the PVA fiber matrix. From the cross section analysis (Fig. 4c&d), PVA and MWCNT/PVA fibers have an average diameter of 340 ± 55 nm and 570 ± 96 nm, respectively. The small bulges and grooves along the MWCNT/PVA fiber indicates that the

MWCNTs are aligned along the fiber axis. The rough surface of the composite fibers is ascribed to the 3D spatial curvature of the MWCNTs and the network formed by the bent MWCNTs themselves. [29] The variation of the fiber diameters is bigger in MWCNT/PVA fiber than the PVA fiber samples.

Nanoindentation was applied for probing the mechanical properties of the PVA and MWCNT/PVA fibers, as this technique provides localized mechanical property comparing to the traditional mechanical testing.[38] Figure 5(a) presents the typical load v.s. displacement curves for PVA and MWCNT/PVA fibers. The indentation was displacement controlled with 80 nm as the maximum indentation depth to minimize the substrate effect, a 5 second loading time, 0 second holding time, and a 5 second unloading time. For the MWCNT/PVA fiber that has an average diameter larger than that of the PVA fiber, the indentation load reaches 25 μN, a 67% increase to the PVA fiber. The reinforcing effect is attributed to the MWCNTs network and the interactions between the MWCNTs and the matrix that help resist bigger deformation of the MWCNT/PVA fiber. Based on Eqs. (1-4), the elastic moduli and hardness of PVA and MWCNT/PVA fibers are calculated to be 1.6 ± 0.3 GPa, and 4.0 ± 1.2 GPa, respectively, shown in Fig. 5(b). The harnesses of PVA and MWCNT/PVA fibers are measured to be 237 ± 79 MPa, and 492 ± 129 MPa, respectively. The 15 wt% MWCNTs exhibits significant improvement in the mechanical property. The relatively larger variations in both elastic modulus and hardness for MWCNT/PVA fibers are most likely due to the spatial positions and density distribution of the MWCNTs in the fibers.

By using the custom-designed micro/nano tensile tester, fracture mechanisms and localized deformation can be investigated. The typical tensile stress and strain curve for the three types of epoxy samples is shown in Fig. 6(a). It is seen from Fig. 6(b) that the epoxy sample reinforced with the MWCNT/PVA parallel fiber arrays has the highest tensile strength of 66 ± 15 MPa, followed by the plain epoxy control sample (54 ± 7 MPa), and the epoxy reinforced with PVA parallel fiber array (40 ± 10 MPa), which is similar to the comparison result of the elastic moduli. As PVA polymer is less stiff than the epoxy for this experiment, the addition of the PVA fiber arrays in the epoxy matrix weakens the overall mechanical property of the composite. During straining, the relatively soft PVA fiber arrays may serve as cushion for energy absorption and blunt the micro crack noses to lower the crack propagation speed. The elongation at break for the epoxy reinforced with the MWCNT/PVA parallel fiber arrays is decreased compared with the failure strain of the plain epoxy. It indicates that the incorporation of MWCNTs in the epoxy matrix creates composites with higher modulus and strength, especially with the array of parallel reinforcing nanofibers in the matrix.

CONCLUSIONS

In this paper, parallel polyvinyl alcohol electrospun nanofibers reinforced by MWCNTs and its reinforced epoxy composite were fabricated, the mechanical characterization was performed. Through AFM analysis, the morphology of the PVA fiber was much smoother and more uniform than the MWCNT/PVA fiber. The elastic moduli and hardness of PVA and MWCNT/PVA fibers from Nanoindentation tests were calculated. The 15 wt% MWCNTs exhibited significant improvement in the mechanical property. Tensile testing showed that the epoxy sample reinforced with the MWCNT/PVA parallel fiber arrays had the highest tensile strength, followed by the plain epoxy control sample, and the epoxy reinforced with PVA parallel fiber array. It was postulated that the addition of the PVA fiber arrays in the epoxy matrix weakened the overall mechanical property of the composite. The elongation at break for the epoxy reinforced with the MWCNT/PVA parallel fiber arrays was decreased compared with the failure strain of the plain epoxy. It indicated that the incorporation of MWCNTs in the epoxy matrix created composites with higher modulus and strength, especially with the array of parallel reinforcing nanofibers in the matrix.

ACKNOWLEDGEMENTS

Funding support is provided by ND NASA EPSCoR FAR0017788.

REFERENCES

[1] Baskaran R, Sarojadevi M and Vijayakumar C T 2011 Unsaturated polyester nanocomposites filled with nano alumina *Journal of Materials Science* **46** 4864-71
[2] Zhou X, Shin E, Wang K W and Bakis C E 2004 Interfacial damping characteristics of carbon nanotube-based composites *Composites Science and Technology* **64** 2425-37
[3] Li X D, Gao H S, Scrivens W A, Fei D L, Xu X Y, Sutton M A, Reynolds A P and Myrick M L 2004 Nanomechanical characterization of single-walled carbon nanotube reinforced epoxy composites *Nanotechnology* **15** 1416-23
[4] Strong L E and West J L 2011 Thermally responsive polymer-nanoparticle composites for biomedical applications *Wiley Interdisciplinary Reviews-Nanomedicine and Nanobiotechnology* **3** 307-17
[5] Loos M R and Schulte K 2011 Is It Worth the Effort to Reinforce Polymers With Carbon Nanotubes? *Macromolecular Theory and Simulations* **20** 350-62
[6] Fiedler B, Gojny F H, Wichmann M H G, Nolte M C M and Schulte K 2006 Fundamental aspects of nano-reinforced composites *Composites Science and Technology* **66** 3115-25
[7] Collins P G, Arnold M S and Avouris P 2001 Engineering Carbon Nanotubes and Nanotube Circuits Using Electrical Breakdown *Science* **292** 706-9
[8] Ko F K, Khan S, Ali A, Gogotsi Y, Naguib N, Yang G, Li C, Shimoda H, Zhou O and Bronikowski M J 2002 Structure and Properties of Carbon Nanotube Reinforced Nanocomposites. In: *43rd AIAA/ASME/ASCE/AHS/ASC Structures, Structural Dynamics, and Materials Conference*, (Denver, CO; UNITED STATES: AIAA)
[9] Iijima S 1991 Helical microtubules of graphitic carbon *Nature* **354** 56-8
[10] Ruoff R S, Qian D and Liu W K 2003 Mechanical properties of carbon nanotubes: theoretical predictions and experimental measurements *C. R. Phys.* **4** 993-1008
[11] Zeng J, Xu X, Chen X, Liang Q, Bian X, Yang L and Jing X 2003 Biodegradable electrospun fibers for drug delivery *J. Controlled Release* **92** 227-31
[12] Ramakrishna S, Jose R, Archana P S, Nair A S, Balamurugan R, Venugopal J and Teo W E Science and engineering of

electrospun nanofibers for advances in clean energy, water filtration, and regenerative medicine *J. Mater. Sci.* **45** 6283-312
[13] Sell S A, Wolfe P S, Ericksen J J, Simpson D G and Bowlin G L 2011 Incorporating Platelet-Rich Plasma into Electrospun Scaffolds for Tissue Engineering Applications *Tissue Engineering Part A* **17** 2723-37
[14] Filatov Y, Budyka A and Kirichenko V 2008 "Electrospinning of Micro- and Nanofibers:Fundamentals in Separation and Filtration Processes". INDA, Association of the Nonwovens Fabrics Industry)
[15] Lee S and Obendorf S K 2007 Use of Electrospun Nanofiber Web for Protective Textile Materials as Barriers to Liquid Penetration *Text. Res. J.* **77** 696-702
[16] Taylor G 1969 Electrically Driven Jets. In: *Mathematical and Physical Sciences*: The Royal Society) pp 453-75
[17] Thompson C J, Chase G G, Yarin A L and Reneker D H 2007 Effects of parameters on nanofiber diameter determined from electrospinning model *Polymer* **48** 6913-22
[18] Dersch R, Liu T Q, Schaper A K, Greiner A and Wendorff J H 2003 Electrospun nanofibers: Internal structure and intrinsic orientation *Journal of Polymer Science Part a-Polymer Chemistry* **41** 545-53
[19] Doshi J and Reneker D H 1995 Electrospinning process and applications of electrospun fibers *Journal of Electrostatics* **35** 151-60
[20] Li D, Wang Y L and Xia Y N 2004 Electrospinning nanofibers as uniaxially aligned arrays and layer-by-layer stacked films *Adv. Mater. (Weinheim, Ger.)* **16** 361-6
[21] Theron A, Zussman E and Yarin A L 2001 Electrostatic field-assisted alignment of electrospun nanofibres *Nanotechnology* **12** 384-90
[22] Deitzel J M, Kleinmeyer J D, Hirvonen J K and Tan N C B 2001 Controlled deposition of electrospun poly(ethylene oxide) fibers *Polymer* **42** 8163-70
[23] Boland E D, Wnek G E, Simpson D G, Pawlowski K J and Bowlin G L 2001 Tailoring tissue engineering scaffolds using electrostatic processing techniques: A study of poly(glycolic acid) electrospinning *Journal of Macromolecular Science-Pure and Applied Chemistry* **38** 1231-43
[24] Zussman E, Theron A and Yarin A L 2003 Formation of nanofiber crossbars in electrospinning *Appl. Phys. Lett.* **82** 973-5
[25] Dai H Q, Gong J, Kim H and Lee D 2002 A novel method for preparing ultra-fine alumina-borate oxide fibres via an electrospinning technique *Nanotechnology* **13** 674-7
[26] Reneker D, Yarin A, Evan E, Kataphinan W, Rangkupan R, Liu W, Koombhongse S and Xu H 2001 *Electrospinning and nanofibers, Book of Abstracts*
[27] Ishii Y, Sakai H and Murata H 2008 A new electrospinning method to control the number and a diameter of uniaxially aligned polymer fibers *Mater. Lett.* **62** 3370-2
[28] Chuangchote S and Supaphol P 2006 Fabrication of aligned poly(vinyl alcohol) nanofibers by electrospinning *J. Nanosci. Nanotechnol.* **6** 125-9
[29] Ge J J, Hou H Q, Li Q, Graham M J, Greiner A, Reneker D H, Harris F W and Cheng S Z D 2004 Assembly of well-aligned multiwalled carbon nanotubes in confined polyacrylonitrile environments: Electrospun composite nanofiber sheets *J. Am. Chem. Soc.* **126** 15754-61
[30] Koski A, Yim K and Shivkumar S 2004 Effect of molecular weight on fibrous PVA produced by electrospinning *Mater. Lett.* **58** 493-7
[31] Zheng H, Du Y M, Yu J H, Huang R H and Zhang L 2001 Preparation and characterization of chitosan/poly(vinyl alcohol) blend fibers *J. Appl. Polym. Sci.* **80** 2558-65
[32] Yao L, Haas T W, Guiseppi-Elie A, Bowlin G L, Simpson D G and Wnek G E 2003 Electrospinning and stabilization of fully hydrolyzed poly(vinyl alcohol) fibers *Chem. Mater.* **15** 1860-4
[33] Ding W, Dikin D A, Chen X, Piner R D, Ruoff R S, Zussman E, Wang X and Li X 2005 Mechanics of hydrogenated amorphous carbon deposits from electron-beam-induced deposition of a paraffin precursor *J. Appl. Phys.* **98**
[34] Oliver W C and Pharr G M 1992 An improved technique for determining hardness and elastic-modulus using load and displacement sensing indentation experiments *J. Mater. Res.* **7** 1564-83
[35] Sneddon I 1965 The relation between load and penetration in the axisymmetric boussinesq problem for a punch of arbitrary profile *International Journal of Engineering Science* **3** 47-57
[36] Li D, Wang Y L and Xia Y N 2003 Electrospinning of polymeric and ceramic nanofibers as uniaxially aligned arrays *Nano Lett.* **3** 1167-71
[37] Zhang Q, Chang Z, Zhu M, Mo X and Chen D 2007 Electrospun carbon nanotube composite nanofibres with uniaxially aligned arrays *Nanotechnology* **18**
[38] Sun Y, Huang Z and Li X 2009 Nanoclay-reinforced Polyacrylamide Composite: Synthesis, Structural and Mechanical Characterization *MRS Online Proceedings Library* **1239** null-null

Figure captions:

Figure 1. Schematic of the electrospinner setup for parallel nanofibers fabrication.

Figure 2. Schematic of top and side views of a dog-bone sample.

Figure 3. AFM height image of parallel electrospun fiber array.

Figure 4. AFM height image of (a) PVA fiber and (b) MWCNT/PVA fiber. AFM cross section view of (c) PVA fiber and (d) MWCNT/PVA fiber.

Figure 5. (a) Representative nanoindentation load *v.s.* displacement curves and (b) Elastic modulus and hardness for PVA and MWCNT/PVA fibers.

Figure 6. (a) Representative tensile stress v.s. strain curve comparison and (b) Tensile strength and elastic modulus comparison for plain epoxy, parallel PVA fiber array reinforced epoxy, and MWCNT/PVA parallel fiber array reinforced epoxy specimens.

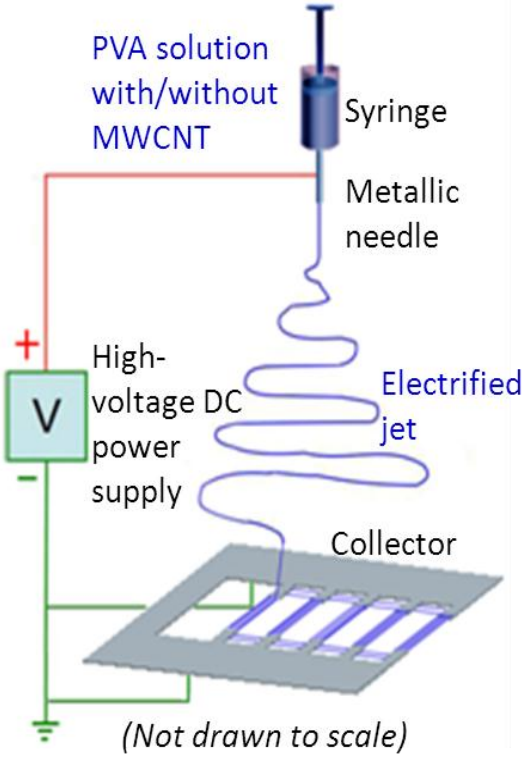

Figure 1.

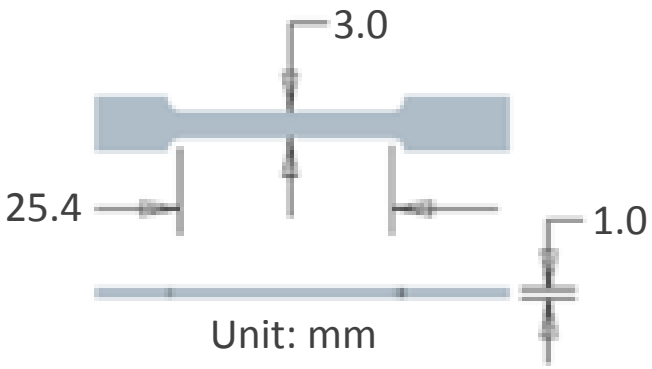

Figure 2.

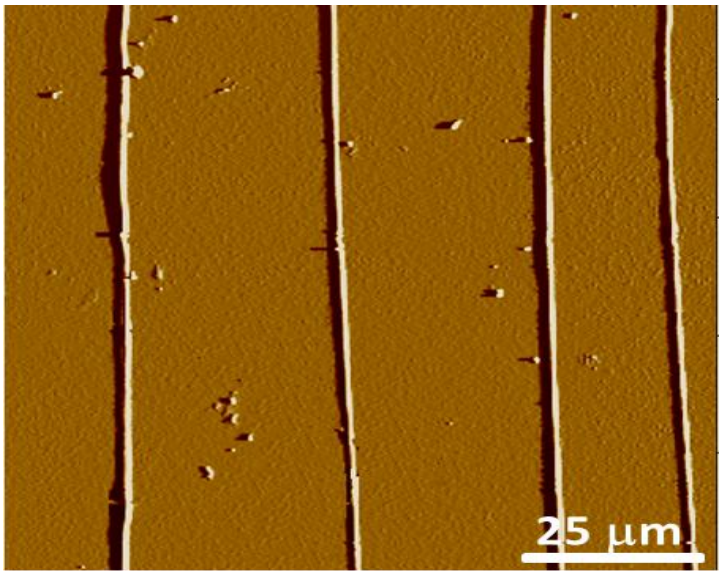

Figure 3.

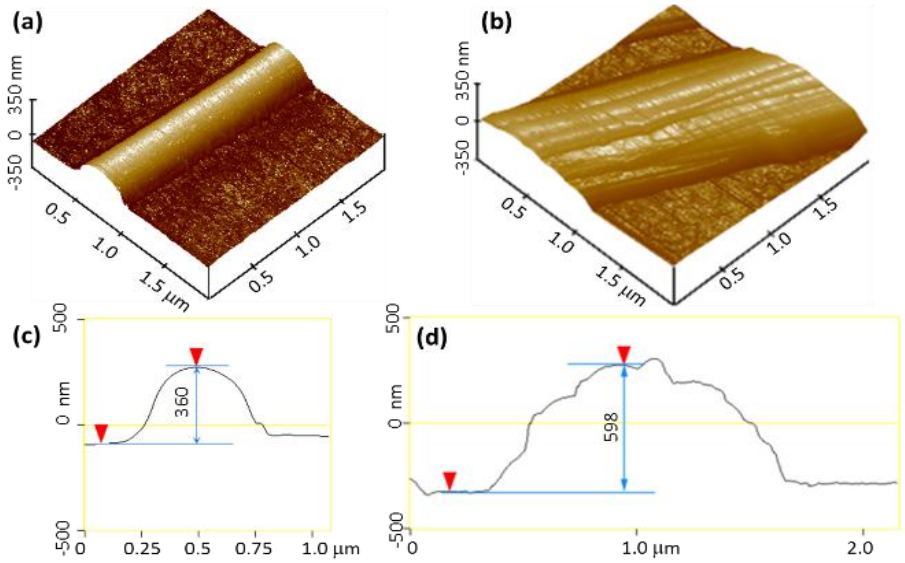

Figure 4.

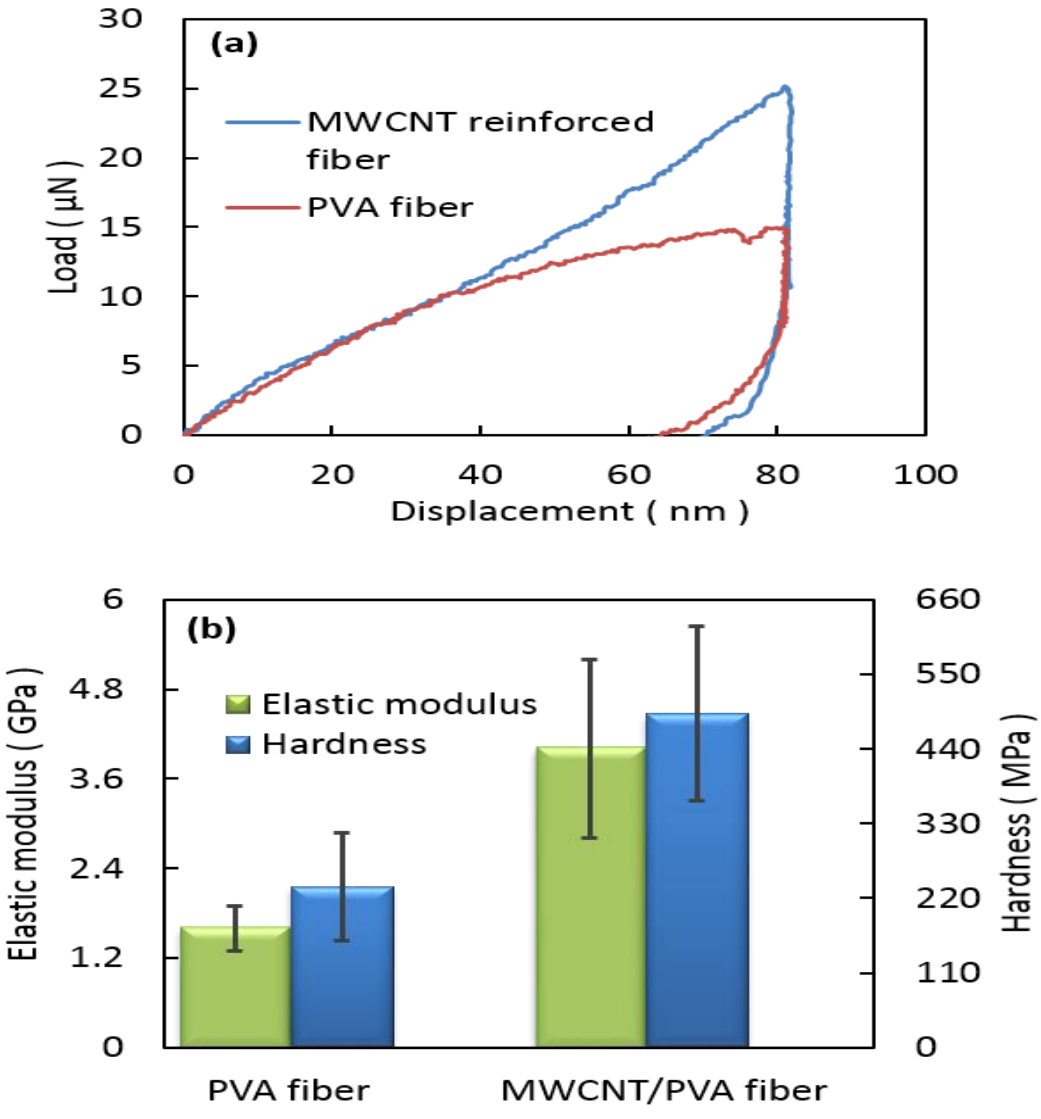

Figure 5.

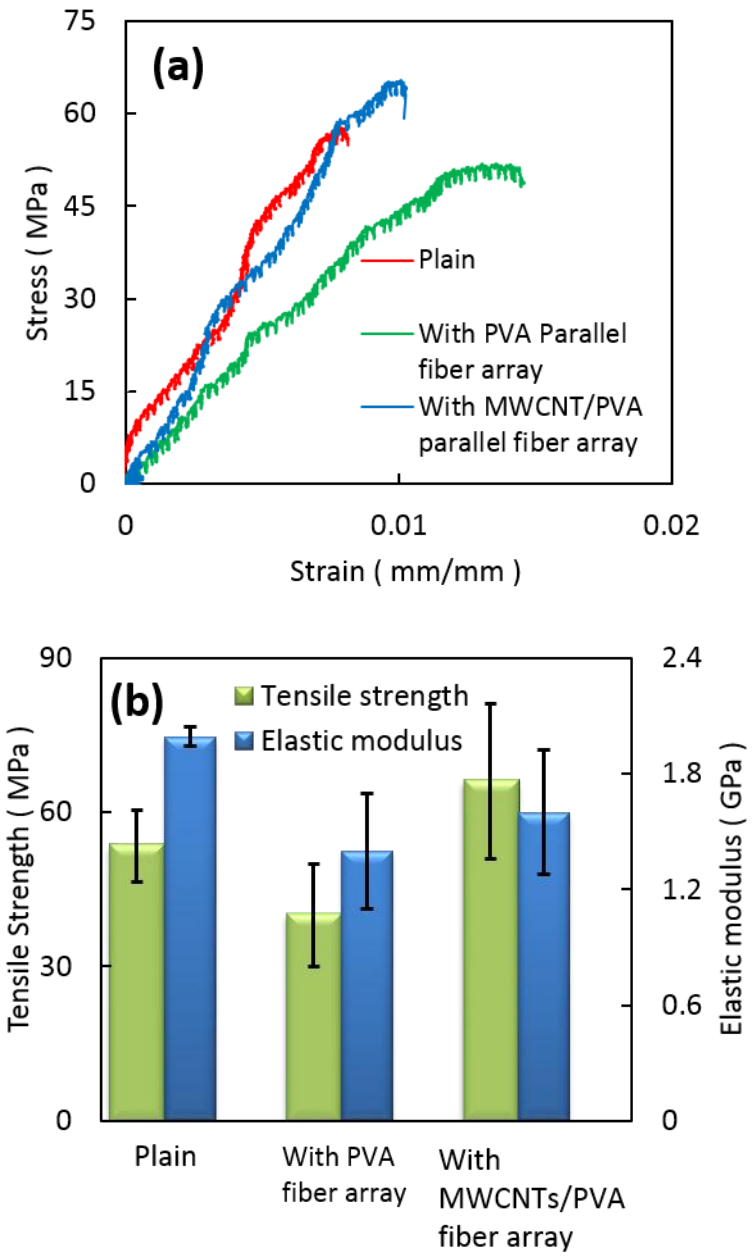

Figure 6.